where

$$g_2 = \frac{E_1}{E_2}\left[\frac{k_2^2+1}{k_2^2-1} + \nu + \frac{M_2 f_3(r_1)}{\beta_1} + E_2 \frac{G_2}{r_1} + g_{m4}(r_1)\right]$$

$$+ \frac{k_1^2+1}{k_1^2-1} - \nu \quad . \tag{66}$$

Similarly, q_1 is found if p is taken as zero; i.e.,

$$q_1 = \frac{E_1 \Delta T (\alpha_1 - k_2 \alpha_2)}{g_2} \quad . \tag{67}$$

Formulating the range in hoop stress $(\sigma_\theta)_r$ at the bore (Equation (56) and using the definition $\alpha_r \sigma_1 = (\sigma_\theta)_r$, we get the following expression for p/σ_1:

$$\frac{p}{\sigma_1} = \frac{2\alpha_r (k_1^2 - 1)^2 g_2}{\left[g_2 (k_1^4 - 1) - 4k_1^2\right]} \tag{68}$$

[Equation (68) is identical in form to Equation (58).]

The pressure-to-strength ratio p/σ_1 is plotted in Figure 58. Comparing this figure with Figure 45 for the multiring container with $\alpha_r = 0.5$, it is evident that both containers have the same limit $p/\sigma_1 \rightarrow 1$ for large wall ratios. However, $\alpha_r = 0.5$ is possible only if $\alpha_m \leqq 0$ as shown in Figure 42. Actually, $\alpha_m = +0.5$ is likely in the pin-segment container if $\alpha_r = 0.5$ because any interference is expected to be lost in taking up slack between pins and holes. In this case, then, $\alpha_r = 0.5$ would mean only one cycle life whereas $\alpha_r = 0.5$ means 10^4 to 10^5 cycles life in the multiring container. If this assembly problem could be eliminated by careful machining and selective fitting of pins, then theoretically with sufficient compressive prestress, the p/σ_1 ratio of the pin-segment container could be made to approach that of the multiring container.

Since no prestress has been assumed for the pin-segment container, $\alpha_r = \alpha_m = 0.35$ for 10^4 to 10^5 cycles as shown by Figure 42. For $\alpha_r = 0.35$, it is found that p/σ_1 is limited to 0.7 at best. Therefore, the maximum pressure in the pin-segment container is p = 0.7 (300,000) = 210,000 psi for 10^4 to 10^5 cycles life.

The stresses in the segments have not yet been considered. High stresses develop around the pin holes. These too limit the pressure in the pin-segment container. Analysis of the stresses in the segments is described in Appendix I. For the purpose of estimating stresses in the segments the interface pressure p_1 is needed. Therefore, plots of p_1/p are provided in Figure 59. It is evident that the interface pressure p_1 is appreciably less than the bore pressure p_1 especially for large k_1 and small k_2.

The pins are analyzed in Appendix II. In order to carry the pressure loading p_1, it is found that the pin-to-segment-diameter ratio must be

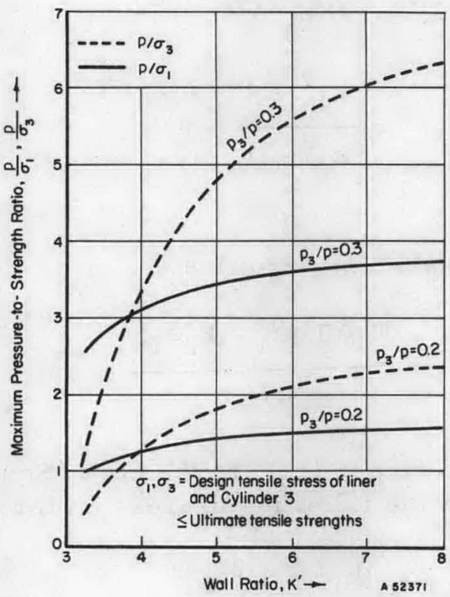

FIGURE 57. EFFECT OF SUPPORT PRESSURE, p_3, ON BORE PRESSURE, p, CAPABILITY FOR THE RING-FLUID-SEGMENT CONTAINER

$\alpha_r = 0.5$, $\alpha_m = -0.5$
$k_1 = 1.5$, $k_2 = 2.0$.

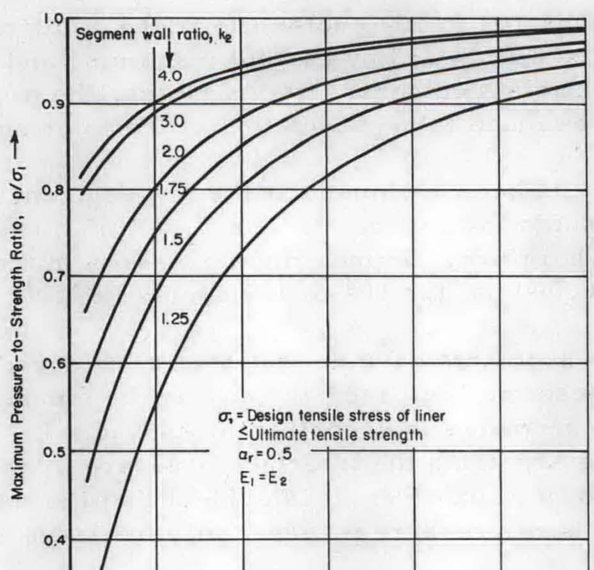

FIGURE 58. MAXIMUM PRESSURE-TO-STRENGTH RATIO, p/σ_1, FOR THE PIN-SEGMENT CONTAINER